12th International Conference on Structural Analysis of Historical Constructions
SAHC 2020
P. Roca, L. Pelà and C. Molins (Eds.)

MULTI-MODAL ANALYSIS OF VIBTATION AND METEOROLOGICAL DATA FOR STRUCTURES ON THE WORLD HERITAGE SITE "BATTLESHIP ISLAND"

NARITO KURATA[1*], KAZUKI TAKAI[2], AKIHIRO TOMIOKA[2], TAKUYA DAIGO[2], SHUNSUKE SARUWATARI[3] AND TAKUJI HAMAMOTO[4]

[1] Graduate School of Technology and Science
Tsukuba University of Technology (NTUT)
3-4-15 Amakubo, Tsukuba city, Ibaraki 305-8520, Japan
e-mail: kurata@home.email.ne.jp, www.tsukuba-tech.ac.jp/english

[2] Akishima Plant
Japan Aviation Electronics Industry, Ltd. (JAE)
3-1-1 Musashino, Akishima city, Tokyo, 196-8555, Japan
email: { takaikz, tomiokaa, daigot }@ jae.co.jp, www.jae.com/en

[3] Graduate School of Information Science and Technology
Osaka University
1-5 Yamadaoka, Suita, Osaka, 565-0871, Japan
email: saru@ist.osaka-u.ac.jp, www.osaka-u.ac.jp/en

[4] Tokyo City University (TCU)
1-28-1 Tamazutsumi, Setagaya-ku, Tokyo, 158-8557, Japan
email: hamamoto325@gmail.com, www.tcu.ac.jp/english

Keywords: Structural Health Monitoring, Vibration Measurement, Meteorological Observation, Accelerometer

Abstract. *This paper reports the results of vibration and meteorological observations of a buildng built on Hashima, Nagasaki, southern part of Japan, which was registered as a World Heritage Site in 2015 [1], and analyzes its dynamic characteristics. Hashima is called "Battleship Island" because its appearance resembles a battleship due to the many buildings standing upon it. The structure contributing most to the battleship appearance is No. 3 Building. An accelerometer and a weather sensor have been installed in No. 3 Building for long-term measurements. Multi-modal analysis of vibration and meteorological data was performed for 5 months, and the dynamic characteristics of No. 3 Building were examined.*

1 INTRODUCTION

Hashima Island in Nagasaki City in the south of Japan was registered as a World Cultural Heritage in 2015 [1]. The island was an offshore city that prospered as an undersea coal mine from the 1800s, and had a population density higher than that of Tokyo. The shape of the island resembles that of a battleship, so it is also referred to as "Battleship Island" (or Gunkanjima).

As a result of the effect of the energy policy from the 1970s onwards the mine closed on 15th January 1974. Thereafter Battleship Island became unoccupied, but a group of building structures that are degrading with time under the severe natural environment remain. The authors have installed various types of sensors on the group of structures on Battleship Island, and are performing monitoring [2]. Building No. 3 contributes most to the resemblance of the silhouette of this island to a battleship. It is the most important among the structures of Battleship Island and must be preserved. A new vibration monitoring system was installed on Building No.3 in May 2019. Building No. 3 is a 4-story reinforced concrete structure; a total of ten accelerometers were installed on each floor on both sides of the rectangular plan, and vibration measurements for the structural health monitoring [3] have been carried out over several months. Every two hours microtremor measurements are performed for 10 minutes, and in addition when vibrations exceeding a certain level occur such as during typhoons and earthquakes, vibration measurements are taken. On the other hand, meteorological sensors were installed on the rooftop of Building No. 3 in October 2017, measuring items such as air temperature, humidity, atmospheric pressure, wind direction, wind velocity, sunlight intensity, and rainfall. This paper presents the results of analysis of the dynamic properties of Building No. 3, obtained from a multi-modal analysis of the vibration data and the meteorological data.

2 NO.3 BUILDING, THE SYMBOL OF BATTLESHIP ISLAND

No. 3 Building on Battleship Island, shown in Fig. 1, is a 4-story reinforced concrete housing complex constructed in 1959. It is located at the highest point on Battleship Island, and is a symbolic building that has a silhouette similar to that of a battleship. The building is relatively new on the island, with little sign of aging and damage. On the rooftop of No.3 Building, a wireless antenna for maritime radio communication with the Battleship Island Museum on the opposite shore, a solar panel, a storage battery, and cameras that capture images of the surrounding area are installed. These serve as communication bases for the monitoring system.

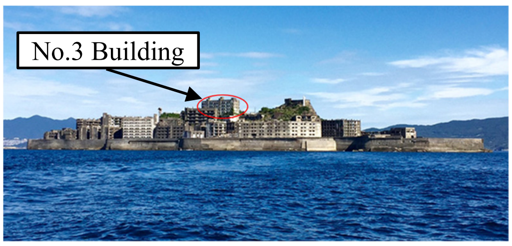

(a) Panoramic View

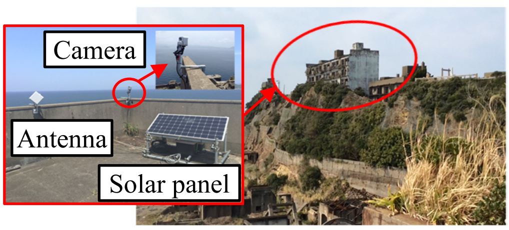

(b) Camera, Energy and Network System

(c) Plan View

Figure 1: No.3 Building

3 VIBRATION MEASUREMENT SYSTEM

Fig. 2 shows the locations of the accelerometers in No. 3 Building [4]. No. 3 Building has a flat, rectangular shape, with a total of 10 acceleration sensors installed on both sides of each floor. Fig. 3 and Table 1 show the system configuration and the specifications of the acceleration sensors [5]. The accelerometers used are JA-70SA manufactured by Japan Aviation Electronics Industry. This accelerometer can measure a wide range of vibrations from microtremors, to strong vibrations during a typhoon or large earthquake. For vibration measurement, a data acquisition device (referred to as a DAQ) having a 16-channel A/D conversion module is used, and synchronization is performed to within 5 μsec by a multiplexer at the preceding stage. Time synchronization is performed by GPS, and the sampling frequency is set to 100Hz. A continuous measurement function that saves 10 minutes of measurement data every 2 hours and a trigger function that stores measurement data when more than a certain level of vibration occurs due to a typhoon or an earthquake are installed. The data stored in the data recorder is transmitted to a data server in the Battleship Island Museum on the opposite shore by a maritime radio communications antenna (see Fig. 1) installed on the rooftop. This data server is accessible via the Internet. Solar panels and storage batteries are installed on the rooftop of the structure to serve as a power source for the vibration measurement system. PCs, the DAQ and accelerometers consume higher power, but they use system power efficiently to provide constant remote monitoring and continuous measurement.

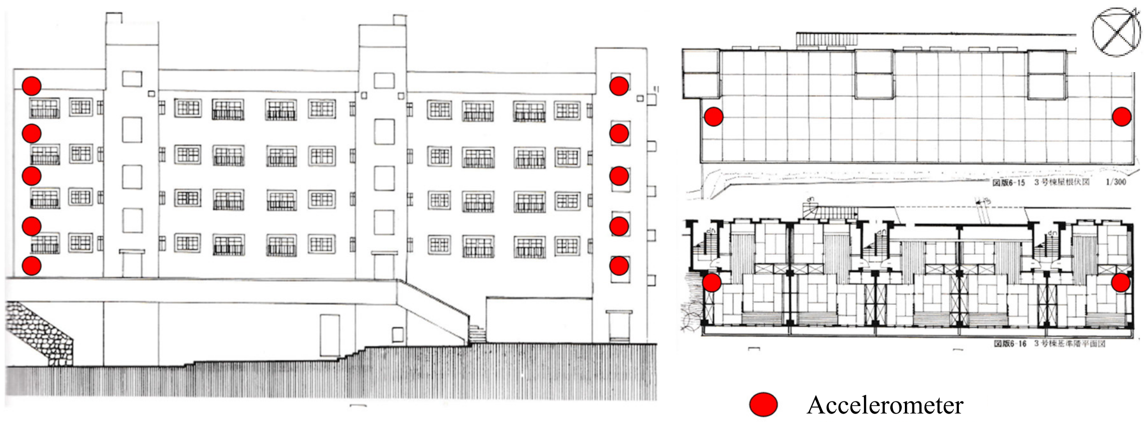

Figure 2: Sensor Location

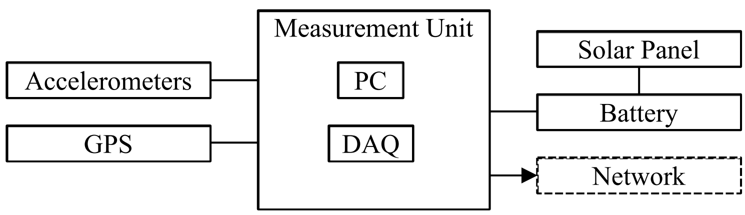

Figure 3: Vibration Measurement System

Table 1: Specifications of Accelerometer

<table>
<tr><th colspan="2">Item</th><th>Units</th><th>JA-70SA</th></tr>
<tr><td colspan="2">Measurement range</td><td>±m/s^2 [±G]</td><td>X,Y axes: ±19.6 or higher [±2]
Z axis: -9.8 - +29.4 [-1~+3]</td></tr>
<tr><td colspan="2">Voltage sensitivity (Note 1)</td><td>V/(m/s^2) [V/G]</td><td>0.2039±5% [2.000±5%]</td></tr>
<tr><td colspan="2">Zero point imbalance (Note 2)</td><td>m/s^2 [mG]</td><td>X,Y axes: within ±0.98 [±100]
Z axis: 9.81±0.98 [-1000±100]</td></tr>
<tr><td colspan="2">Case alignment</td><td>mrad</td><td>within ±20</td></tr>
<tr><td colspan="2">Linearity</td><td>%FS</td><td>within ±2</td></tr>
<tr><td colspan="2">Self-noise (@1~30Hz)</td><td>(m/s^2) rms/$\sqrt{\text{Hz}}$
[Grms/$\sqrt{\text{Hz}}$]</td><td>9.8x10^{-6}
[1x10^{-6}]</td></tr>
<tr><td colspan="2">Frequency response</td><td>Hz(±3dB)</td><td>≥200</td></tr>
<tr><td colspan="2">Voltage sensitivity:temperature coefficient</td><td>ppm/°C</td><td>within ±200</td></tr>
<tr><td colspan="2">Zero point imbalance:
temperature coefficient</td><td>μ(m/s^2)/°C
[μG/°C]</td><td>±1961[±200]</td></tr>
<tr><td rowspan="5">Environmental resistance</td><td>Operating temperature</td><td>°C</td><td>-25~+70</td></tr>
<tr><td>Non-operating temperature</td><td>°C</td><td>-40~+80</td></tr>
<tr><td>Humidity</td><td>%RH</td><td>20~80</td></tr>
<tr><td>Vibration resistance
JIS C60068-2-6</td><td colspan="2">10-60Hz 0.75mm, 60-500Hz 100m/s^2 [10G}
Sinusoidal vibration 10 times for each axis
2H/time</td></tr>
<tr><td>Impact resistance
JIS C60068-2-27</td><td colspan="2">9800m/s^2 [100G] 6ms
Half-sin 3 times for each axis、±direction</td></tr>
<tr><td rowspan="3">Electrical properties</td><td>Power supply voltage</td><td>V(DC)</td><td>±5±0.5</td></tr>
<tr><td>Consumption current</td><td>mA</td><td><17</td></tr>
<tr><td>Output impedance</td><td>Ω</td><td>47typ.</td></tr>
<tr><td rowspan="3">External dimensions</td><td>Width</td><td>mm</td><td>38.6</td></tr>
<tr><td>Depth</td><td>mm</td><td>41.0</td></tr>
<tr><td>Height</td><td>mm</td><td>24.8</td></tr>
<tr><td colspan="2">Mass</td><td>g</td><td>≤100</td></tr>
</table>

4 AUTONOMOUS METEOROLOGICAL OBSERVATION SYSTEM

An autonomous meteorological observation system (Meisei Electric, POTEKA) is installed on the rooftop of No. 3 Building (see Fig. 4) [6]. As shown in Fig. 4(a), the system includes solar panels, storage batteries, a radio communication unit, a weather sensor station, rain gauges, and a base for fixing these devices. The weather sensor station comprises 7 types of sensors (temperature, pressure, humidity, solar radiation, wind direction, wind speed, and precipitation) as shown in Fig. 4(b). Because observation data is updated every minute, it is possible to capture changes in weather conditions in real-time. The weather data is transmitted to the server in real-time via a mobile phone network. Table 2 shows the specifications of the autonomous meteorological observation system, and Table 3 shows the specifications of the weather sensors.

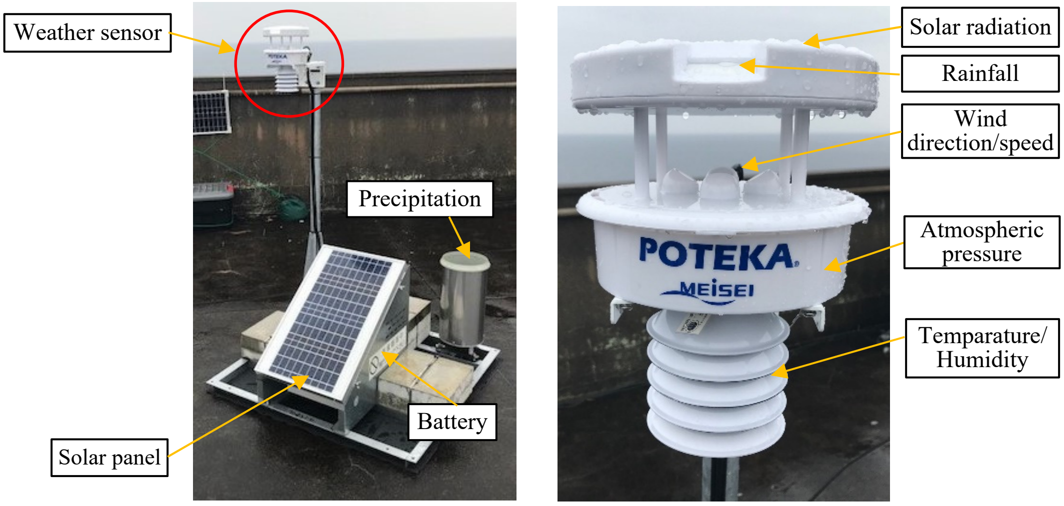

(a) System View (b) Weather Sensor

Figure 4: Meteorological Observation System

Table 2: Specifications of Meteorological Observation System

Observation element of weather sensor	Air temperature, atmospheric pressure, humidity, solar radiation, wind direction, wind speed, rainfall, precipitation
Sampling period	1 second
Statistical interval (output values)	1 min average
Communication interval	60 sec (variable from 10~999 sec)
Data storage	14 days
Solar battery capacity	30 W
Storage cell capacity	18 Ah
Built-in cell	Nickel-hydrogen cell 700mAh
Power interruption backup time	More than 6 hrs.
Operating temperature range	-10°C~+60°C
Wind speed resistance	Average wind speed 60m/s
Communications circuit	3G circuit

Table 3: Specifications of Weather Sensor

Element	Measurement method	Observation range	Precision
Air temperature	Platinum resistor	-50.0~+50.0°C	±0.3°C
Humidity	Capacitive type	0.0~100.0%RH	±5%
Atmospheric pressure	Capacitive type	870.0~1050.0hPa	±0.7hPa
Wind direction	Ultrasonic	0~360°	±10°
Wind speed	Ultrasonic	0.0~30.0m/s	±0.3m/s (0~10m/s) ±5% (10~30m/s)
Solar radiation	Photodiode	0~1400W/m^2	±10%
Rainfall	Capacitive type	0/1	-
Precipitation	Tipping bucket type	Below 200mm/h	±0.5mm (below 20mm) ±3% (above 20mm)

5 ANALYSIS OF VIBRATION AND METEOROLOGICAL DATA

Figs. 5 and 6 show amplitude ratios of Fourier acceleration spectra on the rooftop and the first floor calculated from acceleration data measured for 10 minutes from 12:00 every day, from June 1 to October 18, 2019. As can be seen from the figures, some parts of the data from August 12 to 19 and August 27 to 28 during the measurement period are missing. In each figure, the measurement dates, frequencies, and ratios of Fourier spectra are displayed in 3D and 2D. In addition, the dates of occurrence of three typhoons that caused strong vibrations in No. 3 Building during the measurement period are shown. Fig. 5 shows the analysis results of the long-side components of the sensors installed on the south and north sides of No. 3 Building. From these figures, it can be seen that the first characteristic frequency clearly appears around 6 Hz during strong winds or a typhoon. In addition, characteristic frequencies of higher-order modes can be observed near 17 Hz. Further, if vibration of the building increases due to strong winds or a typhoon, vibration in the high frequency region of 10 Hz or more increases on the south side.

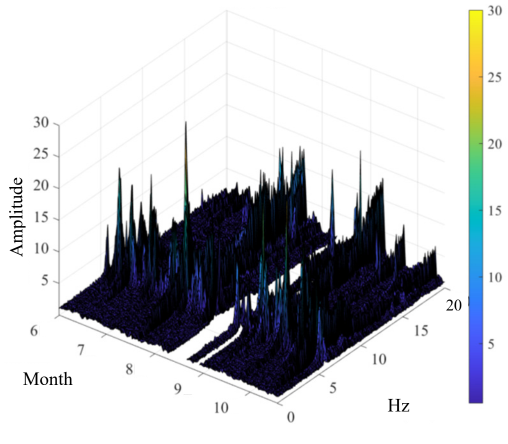

(a) South side (3D)

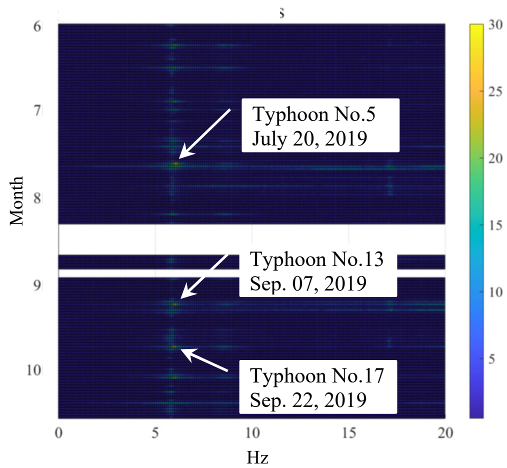

(b) South side (2D)

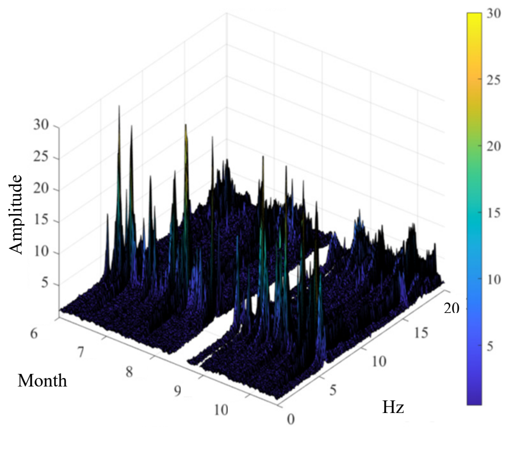

(c) North side (3D)

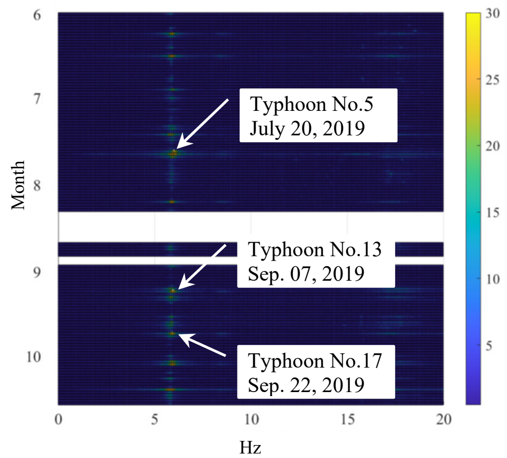

(d) North side (2D)

Figure 5: Fourier amplitude spectrum ratios of the acceleration data (Long-side component)

Fig. 6 shows the analysis results of the short-side components of the sensors installed on the south and north sides of No. 3 Building. From these figures, it can be seen that characteristic frequencies appear at around 9 Hz and 14 Hz in addition to 6 Hz during strong winds or a typhoon. Further, when vibration of the building increases due to strong winds or a typhoon, the vibration on the south side is larger than that on the north side, and on the south side, vibration in the high frequency region of 10 Hz or more increases.

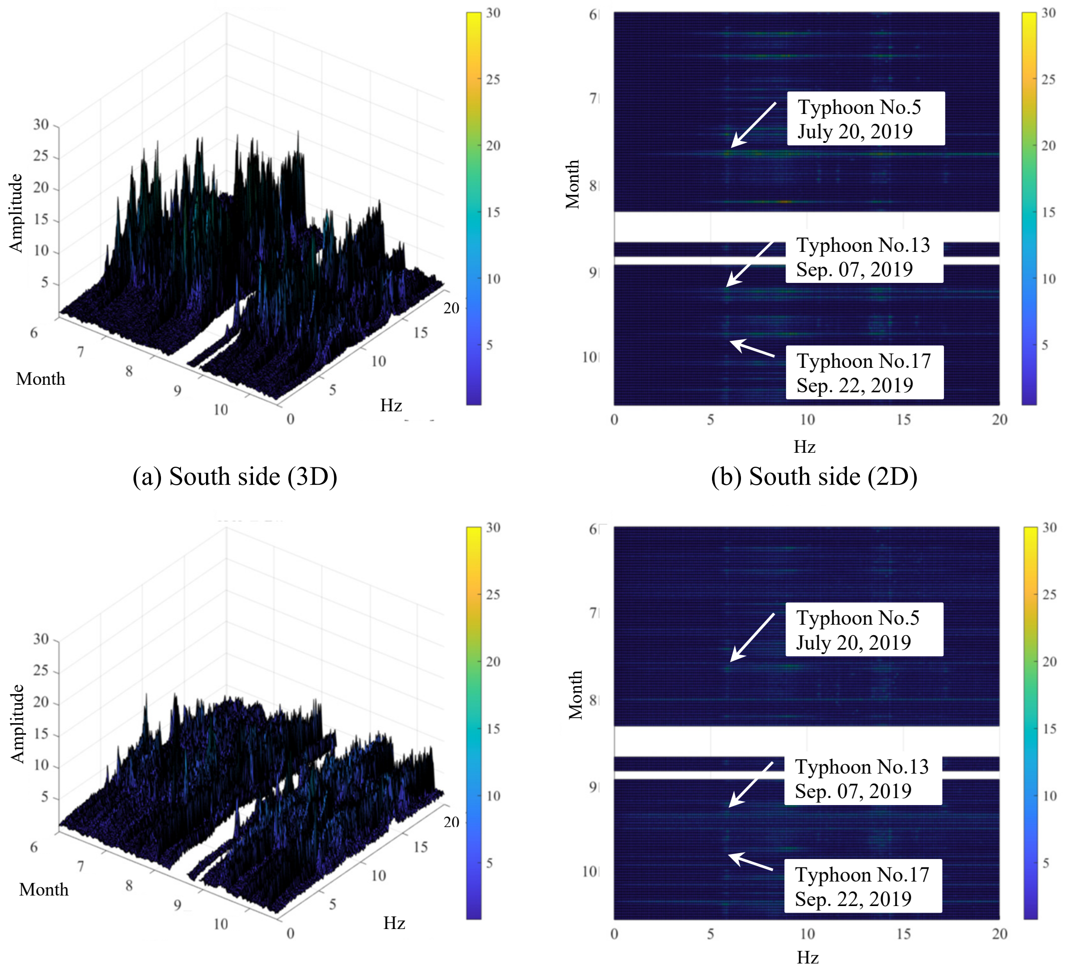

(a) South side (3D) (b) South side (2D)

(c) North side (3D) (d) North side (2D)

Figure 6: Fourier amplitude spectrum ratios of the acceleration data (Short-side component)

Fig. 7 shows the average air temperature and the maximum instantaneous wind speed every 10 minutes, measured from June 1, 2019 to October 18, 2019. This figure also shows the dates of three typhoons that caused large vibrations in No. 3 Building during the measurement period. When the wind speed increases due to a typhoon, the vibration of the building increases, but in No. 3 Building, vibrations other than the characteristic frequencies are excited. As an example, Fig. 8 shows Fourier acceleration spectrum ratio of the roof and first floor in the short-side direction on the south side of the building calculated from acceleration data measured during

Typhoon No. 5. The figure shows the analysis results of data measured for 10 minutes every 2 hours, for 48 hours from 12:00 on July 19 until 12:00 on July 21, or from when Typhoon No. 5 approached until it passed. In the figure, the time zone where the wind speed is high is clearly indicated by the red frame. As the wind speed increases due to the typhoon, the vibration of the building increases, and it can be seen that on the south side of the building, vibrations in the high frequency region of 10 Hz or more are excited.

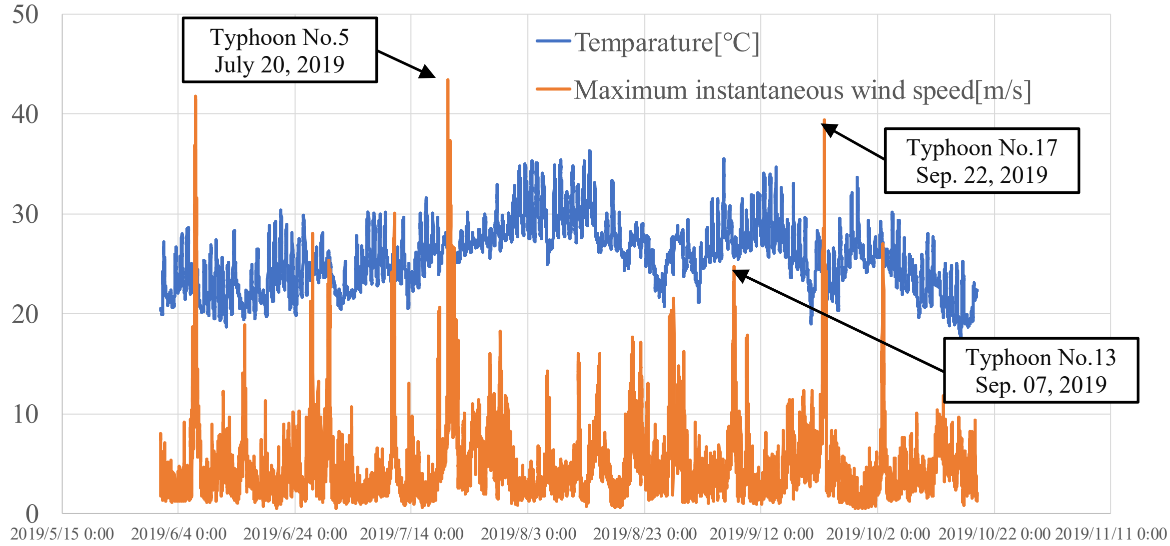

Figure 7: Average air temperature and the maximum instantaneous wind speed

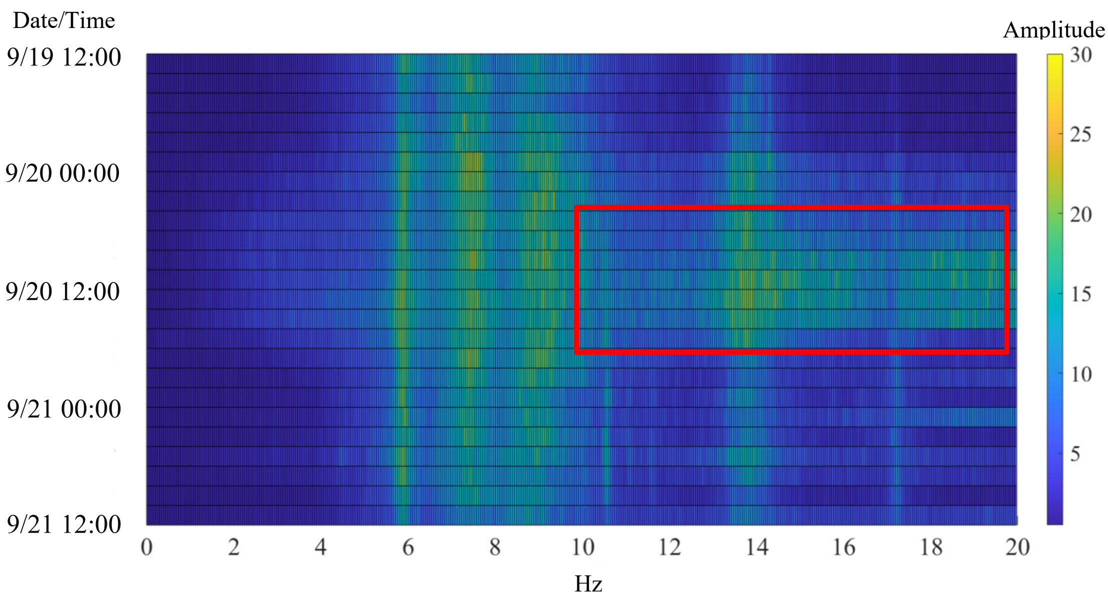

Figure 8: Fourier amplitude spectrum ratios of the acceleration data (Short-side component)

6 CONCLUSIONS

In this paper, vibration measurements and meteorological observations were made on the building of Battleship Island, which is registered as a World Cultural Heritage site, and their dynamic characteristics were analyzed. In the target, No. 3 Building, no change in low-order mode dynamic characteristics due to temperature changes from spring to autumn was observed. It was found that when vibration of the building increased due to strong winds or a typhoon, vibration on the south side was larger than that on the north side, and vibration in the high frequency region was also larger. This suggested that, by observing the fluctuations of low frequency region on the south side after large vibrations occur due to strong winds, a typhoon or an earthquake, it is possible to detect loss of structural stability of the building. In the future, it is planned to continue vibration measurements and meteorological observations for No. 3 Building, and compare the measurement results on a yearly basis including winter.

Acknowledgements. This work was supported by JSPS KAKENHI JP17KT0042 and JP26289194. Nagasaki City cooperated with the installation and measurement on the island. The photos were taken with the special permission of Nagasaki City.

REFERENCES

[1] World Heritage Committee. Decisions adopted by the World Heritage Committee at its 39th session (Bonn, 2015). United Nations Educational, Scientific and Cultural Organization, (2015).

[2] Hamamoto, T., Kurata, N., Saruwatari, S., Kawamoto, K., Tomioka, A. and Daigo, T. Field Test of Change Detection System of Building Group in Preparation for Unexpected Events in GUNKANJIMA. *AIJ J. Technol. Des.* (2018) **24** (57):553-558. in Japanese.

[3] Boller, C., Chang, F-K. and Fujino. Y. (EDS): *Encyclopedia of Structural Health Monitoring,* John Wiley & Sons, 2009.

[4] Akui, Y. and Shiga, H. *Gunkanjima Survey Data Collection (Supplementary Edition)*, Tokyo Denki University Press, 2005. in Japanese.

[5] Tomioka, A., Hamamoto, T., Kurata, N. and Saruwatri, S. Gunkanjima Monitoring Project Part 10: Configuration of MEMS Accelerometer Network. *Summaries of technical papers of annual meeting, Architectural Institute of Japan* (2018), pp. 151-152. in Japanese.

[6] Kurata, N., Sasaki, K., Saruwatari, S., Hamamoto, T. and Tomioka, A. Gunkanjima Monitoring Project Part 11: Autonomous Weather Sensor System installed at the No.3 Building. *Summaries of technical papers of annual meeting, Architectural Institute of Japan* (2018), pp. 83-84. in Japanese.